

# Sample handling concept for in-situ lunar regolith analysis by laser-based mass spectrometry

Peter Keresztes Schmidt  
Space Research and Planetary  
Sciences,

Physics Institute, University of Bern,  
Sidlerstrasse 5, 3012 Bern,  
Switzerland  
peter.keresztes@unibe.ch

Timothy Bandy  
Space Research and Planetary  
Sciences,

Physics Institute, University of Bern,  
Sidlerstrasse 5, 3012 Bern,  
Switzerland  
timothy.bandy@unibe.ch

Michael Althaus  
Space Research and Planetary  
Sciences,

Physics Institute, University of Bern,  
Sidlerstrasse 5, 3012 Bern,  
Switzerland  
michael.althaus@unibe.ch

Simon Studer  
Space Research and Planetary  
Sciences,

Physics Institute, University of Bern,  
Sidlerstrasse 5, 3012 Bern,  
Switzerland  
simon.studer@unibe.ch

Marek Tulej  
Space Research and Planetary  
Sciences,

Physics Institute, University of Bern,  
Sidlerstrasse 5, 3012 Bern,  
Switzerland  
marek.tulej@unibe.ch

Sébastien Hayoz  
Space Research and Planetary  
Sciences,

Physics Institute, University of Bern,  
Sidlerstrasse 5, 3012 Bern,  
Switzerland  
sebastien.hayoz@unibe.ch

Patrik Mändli  
Space Research and Planetary  
Sciences,

Physics Institute, University of Bern,  
Sidlerstrasse 5, 3012 Bern,  
Switzerland  
patrik.maendli@unibe.ch

Benoît Gabriel Plet  
Space Research and Planetary  
Sciences,

Physics Institute, University of Bern,  
Sidlerstrasse 5, 3012 Bern,  
Switzerland  
benoit.plet@unibe.ch

Olivier Studer  
Space Research and Planetary  
Sciences,

Physics Institute, University of Bern,  
Sidlerstrasse 5, 3012 Bern,  
Switzerland  
olivier.studer@unibe.ch

Andreas Riedo  
Space Research and Planetary  
Sciences,

Physics Institute, University of Bern,  
Sidlerstrasse 5, 3012 Bern,  
Switzerland  
andreas.riedo@unibe.ch

Daniele Piazza  
Space Research and Planetary  
Sciences,

Physics Institute, University of Bern,  
Sidlerstrasse 5, 3012 Bern,  
Switzerland  
daniele.piazza@unibe.ch

Matthias Blaukovitsch  
Space Research and Planetary  
Sciences,

Physics Institute, University of Bern,  
Sidlerstrasse 5, 3012 Bern,  
Switzerland  
matthias.blaukovitsch@unibe.ch

Sven Riedo  
Space Research and Planetary  
Sciences,

Physics Institute, University of Bern,  
Sidlerstrasse 5, 3012 Bern,  
Switzerland  
sven.riedo@unibe.ch

Michael Bieri  
Space Research and Planetary  
Sciences,

Physics Institute, University of Bern,  
Sidlerstrasse 5, 3012 Bern,  
Switzerland  
michael.bieri@unibe.ch

Peter Wurz  
Space Research and Planetary  
Sciences,

Physics Institute, University of Bern,  
Sidlerstrasse 5, 3012 Bern,  
Switzerland  
peter.wurz@unibe.ch

**Abstract**—We present the current progress in developing a reflectron-type time-of-flight laser ablation ionization mass spectrometer (RTOF-LIMS) to allow for direct sensitive microanalysis of lunar regolith grains *in situ* on the lunar surface. The LIMS system will operate in the lunar south pole region on a CLPS mission within NASA's Artemis program.

The concept for the regolith sample handling system, which is based on a carousel disk system with a cavity to hold the sample material, will be discussed in detail. Rotating the disk takes care of transporting the sample material from the sample inlet, into which a sample delivery system of the CLPS platform deposits the regolith, to the analysis position below the mass analyzer entrance and, subsequently, disposing the material after analysis is completed. Sample preparation is achieved by passive brushes and a shaping tool to create a sample surface with the necessary planarity. Accurate control of these parameters is important to ensure consistent laser ablation conditions during sample analysis and thus reproducible chemical composition determination of the sample material. The new sample handling system design has an improved acceptance range for larger

regolith grain sizes up to  $\sim 1$  mm  $\varnothing$ . This in turn reduces a possible sampling bias and should lead to a more representative analysis of the regolith's chemical composition. Sample disposal is realized by another set of brushes to clean out the cavity and to allow for new sample material to be deposited.

To verify the feasibility of the sample handling concept and guiding the development thereof, laboratory experiments on a lunar regolith simulant were conducted using a prototype LIMS system. This prototype system has capabilities representative of the flight instrument currently in development regarding the mass analyzer and optical sub-system. The laboratory and flight optical sub-system is based on a microchip Nd:YAG laser system ( $\sim 1.5$  ns pulse width,  $\lambda = 532$  nm, 100 Hz laser pulse repetition rate, laser irradiance  $\sim 1$  GW/cm<sup>2</sup>), and custom-made laser optics to achieve a focal spot on the sample surface of  $\sim 20$   $\mu$ m. Consequently, the conducted measurements can serve as a qualification baseline for the flight instrument during ground-based tests.

## TABLE OF CONTENTS

<b>1. INTRODUCTION .....</b>	<b>2</b>
<b>2. DESCRIPTION OF THE SAMPLE HANDLING SYSTEM CONCEPT .....</b>	<b>2</b>
<b>3. VALIDATION OF THE SAMPLE HANDLING SYSTEM CONCEPT .....</b>	<b>5</b>
<b>4. SUMMARY .....</b>	<b>8</b>
<b>ACKNOWLEDGEMENTS .....</b>	<b>8</b>
<b>REFERENCES.....</b>	<b>8</b>

## 1. INTRODUCTION

An instrument based on laser ablation ionization mass spectrometry (LIMS) for the chemical analysis of lunar regolith is currently under development. LIMS consist of a mass analyzer coupled to a pulsed laser system. The laser beam is focused onto the sample surface to obtain irradiances in the range of MW/cm<sup>2</sup> to TW/cm<sup>2</sup>. This causes ablation of the sample material, and partial atomization and simultaneous ionization thereof [1]. Our LIMS instrument shall operate on a robotic lander platform to conduct autonomous *in-situ* measurements of the mineralogical, element and isotope composition of lunar surface material.

Our LIMS instrument is being developed for a mission within the Commercial Lunar Payload Services (CLPS) framework, which is a part of NASA's Artemis program. The lunar south pole region is being considered as landing site.

Regolith, the targeted sample material of our CLPS-LIMS instrument, covers the lunar surface with a thickness of 5 m to 10 m, depending on location [2], [3]. The regolith's grain size distribution could be inferred from regolith returned during the Apollo missions. About 90 wt% is larger than 10  $\mu$ m, 50 wt% larger than 100  $\mu$ m and 10 % larger than 1 mm [4]. Being an electrical insulator and with no protective lunar magnetosphere, the bombardment of the regolith with charged solar particles leads to electrostatic charging thereof [5]. When designing an instrument for operation on the lunar surface, such properties must be considered during the design phase. Furthermore, selection procedures for the correct grain size fraction of the measurement procedure must be implemented. Electrostatic charging of the sample material can have an influence on the instrument or cause contamination of surfaces, that ought to be clean of regolith [6]. In this contribution, we discuss how this is handled within the design of our CLPS-LIMS instrument and provide experimental results based on measurements conducted with lunar regolith analogue.

LIMS as a chemical analysis technique is suitable for direct determination of element composition and isotope ratios of the sample material, such as lunar regolith [1], [7], [8]. It is based on the ablation and subsequent ionization of the solids caused by a high-irradiance pulsed laser beam. The generated ions are separated according to their mass-to-charge ratio ( $m/z$ ) and subsequently detected.

Our CLPS-LIMS instrument is based on a reflectron-type time-of-flight mass spectrometer ion-optical design (RTOF-MS) [9]–[11]. Laser ablation/ionization is accomplished by a frequency doubled Nd:YAG microchip laser ( $\lambda = 532$  nm,  $\tau \sim 1.5$  ns, 100 Hz pulse repetition rate). Positive ions in the ablated material are accelerated into the mass analyzer. For a more complete description of the CLPS-LIMS instrument and its subunits we refer the reader to the published design study [12].

Changes in the mission profile of CLPS-LIMS, namely the addition of a sample delivery system at the CLPS platform for sample collection from the lunar surface, resulted in a significant redesign of the instruments sample handling system (SHS), which is presented in the first part of this contribution. The concept design was validated and guided by laboratory experiments, which are described in the second part of this contribution.

*Instrument Overview*— The CLPS-LIMS system consists of two main parts, namely the Spectrometer Unit (SMU) and the Electronic Unit (ELU). In Figure 1 an overview of the current SMU design is shown. The SMU carries of the optical sub-system (OSS) on the top, which houses the laser source and the necessary beam shaping optics to generate a focused laser spot on the sample surface. The mass analyzer (MA) is mounted below the OSS and above the SHS.

All components of the instrument are attached to an ultra-stable structure made of sandwich panels with near-zero CTE CFRP face sheets and aluminum honeycomb, which acts also as the spacecraft interface.

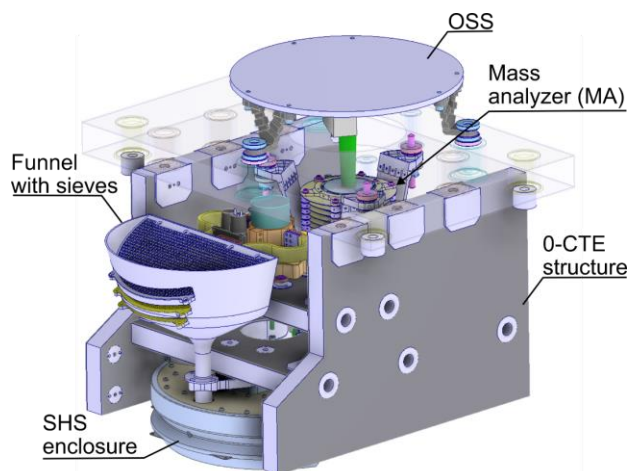


**Figure 1: Overview of the current SMU design of the CLPS-LIMS instrument.**

## 2. DESCRIPTION OF THE SAMPLE HANDLING SYSTEM CONCEPT

The CLPS mission profile foresees split responsibilities between sample collection from the lunar surface and delivery to a defined interface at the CLPS-LIMS instrument, and the subsequent sieving and fine manipulation of the sample material to prepare it for LIMS analysis. The CLPS

lander platform will provide the sample delivery for the CLPS-LIMS instrument.

The external sample delivery system is required to provide a continuous flow or batched drops of 50–100 cm<sup>3</sup> of regolith with grain sized no larger than 5 mm.

The LIMS SHS accepts the collected material from the external sample delivery system (e.g., a robotic arm with a bucket end effector), sieves and shapes the material into an appropriate form for LIMS analysis. Subsequently, it presents the sample to the mass spectrometric system.

A 3D CAD drawing of the SHS’s current design iteration is shown in Figure 2.

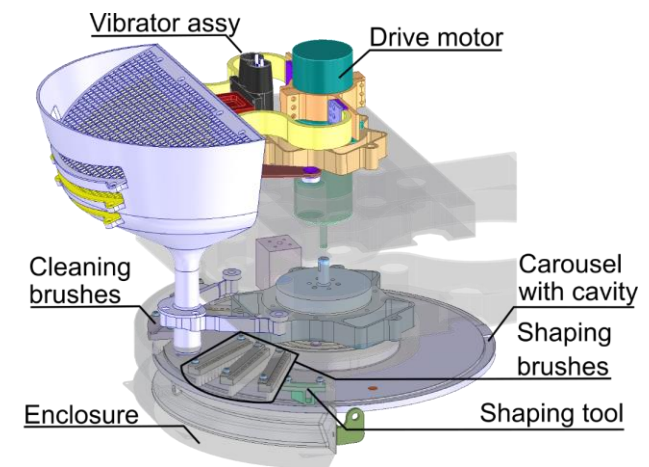


**Figure 2: Close-up view of the sample carousel structure.**

Conceptually, the SHS is built around a rotating sample carousel, which has an approximately 5 mm wide and 1.5 mm deep cavity along its outer edge. The externally delivered sample material is guided through a funnel structure into this cavity while the carousel is rotating counterclockwise. Following the sample deposition, a set of three brushes guides potentially spilled material from the carousel’s main body towards the cavity. To enhance this process, the brushes are mounted rotated into the direction of rotation of the sample carousel. The brushes extend over the cavity as a first step in forming the sample surface and evenly distributing the sample material. For this purpose, the distance between the lower edge of the brushes and the carousel surface decreases across the set of brushes.

After the coarse shaping of the sample material by the brushes, an additional shaping tool further compresses the material and creates a surface with reduced roughness and porosity.

Rotating the carousel further, the now prepared sample material is moved to the measurement position of the CLPS-LIMS instrument. The sample is periodically advanced during analysis to present new material to the mass analyzer and avoid signal degradation due to displacement of the material caused by the laser-matter interaction and consumption of the sample material due to ablation.

After mass spectrometric analysis, the sample material is transported to the disposal structure. Here, another set of brushes removes the regolith from the cavity, making it ready to accept new sample material from the funnel. To aid the sample removal process, the sample cavity wall height is asymmetric with the outer wall being only 0.75 mm high. The brushes force the material over the outer edge of the sample cavity. Note, that a complete removal of sample material from the cavity is not necessary, since only the upper tens of micrometers of the sample material surface are investigated by LIMS.

Disposed sample material falls, by gravitational influence, to the bottom of the instrument enclosure, and passes through a slot present in the enclosure back onto the lunar surface. The slot is protected by a labyrinth structure to minimize radiative heat exchange between the inner part of the instrument and the lunar surface, hence the impact on the SMU’s thermal design is kept minimal. This assures minimal accumulation of disposed sample material inside the instrument enclosure.

Actuation of the sample carousel is performed by a phySpace 32 stepper motor (Phytron GmbH, Gröbenzell, Germany), allowing for precise positional control of the rotation. A planetary gearbox is mounted onto the motor housing to increase effective torque of the carousel and reduce the rotation speed to the required levels. The pre-loaded drive bearings of the sample carousel are protected from lunar regolith using a labyrinth sealing system. Figures of merit of the drive system’s current baseline design are listed in Table 1.

**Table 1: Current figures of merit of the SHS drive system.**

No. of steps per motor axle revolution	200 steps/rev
Drive motor torque	15 mNm
Total gear ratio	1:200
Carousel torque	3 Nm
Linear step size along sample cavity	14 µm

The torque requirements have not been experimentally verified yet and are at this time best estimates. A bread-board design of the carousel system is currently being built to accurately determine the needed torque to advance the sample material through the sample shaping and cavity cleaning sections of the carousel structure.

The minimal step size, with which the sample material can be advanced with, is given by the approximate diameter of the laser focus and thus the diameter of the analyzed area by the LIMS instrument. This has the advantage of not having to step the motor multiple times to reach a new sample area while also not wasting precious lunar sample material by having steps larger than the analyzed area. Consequentially, this reduces the duty cycle of the motor and thus power consumption and heat dissipation.

For initial position referencing a Hall effect or optical sensor is foreseen to be mounted to the top side of the carousel. No active position feedback is needed to keep track of the current rotation position of the carousel due to the fixed step sizes of the motor after initial referencing of the carousel position.

*Sample surface quality and shaping tool*—For optimal analysis of the lunar regolith with the LIMS instrument a sample surface with a defined height and small corrugation is necessary. Due to the ion optical design of the MA, the sample surface must have a distance of  $(0.6 \pm 0.6)$  mm from the opening of the mass analyzer to achieve good collection of the ions generated the laser ablation. Furthermore, the required irradiance of the focused laser beam for sample ablation and ionization is only achievable in the same range. To account for any possible misalignment of the laser focus and the mass analyzer with respect to the nominal sample surface caused by thermo-mechanical distortion or external forces during launch and or landing, the sample planarity shall be better than  $\pm 0.2$  mm when presented to the mass analyzer. The carousel will be designed to fulfill this constraint over full rotations of the carousel.

In Figure 3 the currently considered schematic designs for the sample shaping tools are shown. After forcing the regolith through beneath the shaping tool, the material should have the necessary planarity and reduced porosity required for analysis by LIMS. The appropriate tool design is currently being investigated using the SHS breadboard system (Figure 4). The knife edge tool (3) is currently favored due to its simple mechanical design. Due to the possibility of large grains getting stuck between the knife edge and the cavity, alternative solutions are being considered if the knife edge tool is proven to be not feasible. These might be a flexible Teflon lip tool (1) or a brush tool (2). Using a brush or Teflon lip could pose problems regarding insufficient compression and poor surface quality.

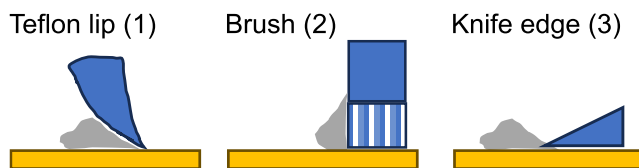


**Figure 3: Schematic depiction of the shaping tools considered for the SHS. The carousel is shown in yellow with its nominal direction of rotation being to the right.**

*Launch lock*—Unwanted movement of the carousel during launch, transit and landing are avoided by locking the carousel using a launch-lock pin. During the commissioning phase on the lunar surface, a spring-loaded, shape-memory alloy triggered pin puller is actuated allowing for motor-driven rotation of the carousel.

#### Funnel

The funnel serves as a drop zone for the CLPS platform's sample delivery system into which the collected lunar regolith is placed. Since the LIMS instrument is designed to

handle only regolith with grain sizes of 1 mm and smaller, three sieves with decreasing mesh sizes (5 mm  $\rightarrow$  2 mm  $\rightarrow$  1 mm) are integrated into the funnel. It is defined that the sample delivery system is allowed drop regolith with grain sizes up to 5 mm to avoid clogging or damaging the sieves.

The sieves are slanted downwards away from the instrument body and cutouts in the funnel allow for the discarding of the unwanted fractions of lunar regolith.

To aid sieving and transport of the regolith material, an eccentric vibrator actuated by a brushed DC motor is attached to the funnel. The vibration frequency can be changed by increasing or decreasing the motor's rotation speed. This allows to tune the regolith flow through the funnel and hence onto the sample carousel. A voice coil vibrator has been considered, but due to the more complex control electronics required, the DC motor-based solution was chosen.

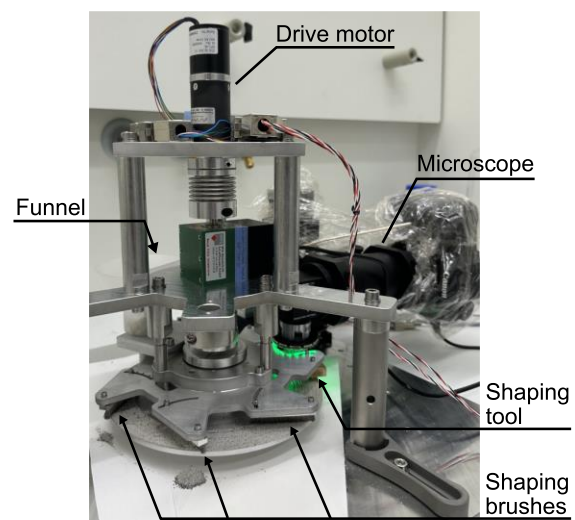


**Figure 4: Sample handling system (SHS) breadboard to test different shaping tools and a custom microscope to quantitatively evaluate the resulting sample planarity.**

#### Reference Samples

For post-landing checkout and calibration purposes two reference samples are foreseen. They are placed within a section of the outer perimeter of the sample carousel for which the sample cavity is interrupted. These samples will be analyzed first and, according to nominal planning only once, during the commissioning since their surface can become contaminated with lunar regolith during operations (see discussion below).

The first reference sample is a monolithic piece of AISI 316 L / 1.4435 stainless steel, which is glued into its respective cavity on the sample carousel. This material has been studied extensively with the laboratory prototype LIMS instruments and thus offers good comparability and evaluation of the performance of the LIMS system when deployed on the lunar surface. In addition, the well-defined surface of the steel reference sample reduces effects on the LIMS measurement stemming from deviations of the sample



surface height, thus simplifying optimization procedures. Due to a low ablation rate of the steel, extensive measurement sequences (> 50'000 shots) can be performed on a single location of the sample without degradation of the spectral characteristics, reducing the size of the needed steel reference sample.

The second reference sample is lunar regolith analogue material pressed to a pellet. It is used for optimizing the operating parameters of the LIMS instrument (e.g., laser pulse energy, voltages applied to the ion optical system) as well as deriving calibration factors for all relevant species by using this matrix matched reference standard for the lunar regolith. Due to the low structural integrity of such a pressed pellet, it is sealed with a lid when the sample carousel is in its launch position.

When one of the reference samples is requested to be analyzed, the carousel is rotated in its nominal direction until the reference sample material is at the measurement location. This procedure is even feasible if the funnel still contains sample material while the reference materials pass below it. The last shaping brush is flush with the reference sample surface, thereby removing any potential regolith coverage that was deposited on top of the reference sample. If contamination of the reference sample is observed during subsequent analysis, one or multiple full rotations of the sample carousel can be initiated. This will empty the funnel and additionally the reference samples pass below the disposal and shaping brushes for additional cleaning of the surfaces.

#### *Disposal of sample material and contamination control*

Analysis of the lunar regolith with the CLPS-LIMS system consumes only a negligible amount of the sample material, in laser ablation mode in the range of fg – pg per laser shot [13], [14]. Most of the sample material entering the system will be disposed of unaltered. After analysis, the remaining material is discarded through a well-defined opening at the bottom of the instrument. Thus, appropriate positioning of the CLPS-LIMS instrument on the spacecraft has to be implemented to avoid potential contamination of other payloads with lunar regolith.

During sample material loading through the funnel and the sieving structure, regolith with too large grain sizes is removed through the openings at the front of the funnel (openings to the left, Figure 2). The disposal opening of the instrument and the funnel structure are in the XY-plane within ~60 mm of each other. No discharge from other parts of the instrument is expected.

To avoid contamination of the instrument with regolith other than introduced through the funnel, the instrument's internal elements are protected partly by the structural assembly itself. The remaining openings are covered by epoxy impregnated glass fiber sheets. The second layer of protection consists of the multi-layer insulation (MLI) covering the instrument. Defined openings with sealed perimeters are foreseen for the funnel, which must be external of the MLI and the sample

discharge opening. Internally the sections of the carousel where sample manipulation and shaping take place, are shielded by a top cover to contain regolith fines.

### **3. VALIDATION OF THE SAMPLE HANDLING SYSTEM CONCEPT**

In this section we describe the experiments conducted on a prototype laboratory LIMS system and our findings, which helped guide the engineering choices made during the design phase of the SHS. All validation experiments were conducted using the lunar highlands simulant LHS-1 (Exolith Lab, Oviedo, FL, USA) as sample material. It is a high-fidelity lunar simulant, matching the chemical and geotechnical properties of lunar regolith found in the lunar highlands [15]. The mineral composition of the lunar simulant material is: SiO<sub>2</sub> (51.2 %), TiO<sub>2</sub> (0.6 %), Al<sub>2</sub>O<sub>3</sub> (26.6 %), FeO (2.7 %), MnO (0.1%), MgO (1.6%), CaO (12.8 %), Na<sub>2</sub>O (2.9 %), K<sub>2</sub>O (0.5 %), P<sub>2</sub>O<sub>5</sub> (0.1 %), and others (0.4 %) as given by XRF measurements. It is expected for the regolith found in the lunar south pole region to exhibit similar properties [16].

#### *Stability of lunar regolith within the sample cavity*

The lunar regolith must be able to keep its shape within the

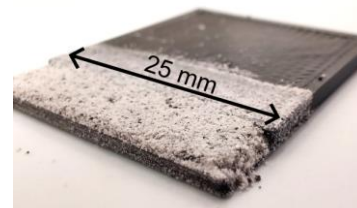


**Figure 5: LHS-1 analogue material filled and shaped within a 3D printed linear strip of the carousel cavity profile (front). Some material is present outside of the cavity profile.**

cavity of the sample carousel after its manipulation with the shaping brushes and the shaping tool for the correct functioning of the SHS. This is to ensure that the sample surface is still suitable for measurement using the LIMS instrument after the material is transported from the sample ingestion section to the analysis location.

To test this, a 3D printed linear section with matching dimensions of the current cavity design was manufactured. It was coarsely filled with LHS-1, emulating the filling process the funnel and subsequently flattened to the height of the inner cavity wall using an L-shaped tool. The prepared cavity strip is shown in Figure 5. The sample retained its shape with no material flowing over the lower outer edge of the cavity. From optical inspection, the sample surface showed no major openings or cavities, and the sample planarity was compatible with the requirements for analysis using LIMS.

It remains to be tested whether potential vibrations during sample transport are degrading the sample surface quality, possibly requiring higher compression of the material. The cohesion of the used LHS-1 material is given with 0.311 kPa [15], whereas lunar regolith is expected to have cohesion

values of 0.1 – 1 kPa [17] as encountered during the Apollo missions. With the cohesion of LHS-1 being on the lower end of the lunar regolith cohesion, using LHS-1 can be seen as a worst-case scenario. In addition, the higher angle of repose of regolith (LHS-1: 47.5°, lunar regolith: 58°) and the lower gravity on the Moon will lead to a more stable outer sample edge [18].

#### *LIMS measurements of lunar regolith simulant*

Measurements of the lunar analogue material were performed using a laboratory space prototype LIMS instrument [19]. For these measurements the LHS-1 sample material was filled into a AISI 316 L / 1.4435 stainless steel sample holder having 1 mm deep cavities. The prepared sample material in the holder is shown in Figure 6. To ensure sufficient planarity, the surface was levelled by moving the edge of a spatula over the sample material. Explicit compression of the material was avoided to simulate the worst-case scenario regarding porosity of the sample surface.

Optimization of the ion-optical voltage set of the ion-optical system was performed using the stainless steel holder itself as sample material. Ion-optical parameters were tuned to maximize signal intensity and mass resolution ( $m/\Delta m$ ). This assures maximal sensitivity of the instrument and high spectral quality at the same time.

The sample planarity is a key factor for the quality of the obtained mass spectra. Because of the on-axis extension of the laser focus (Rayleigh length) there is a direct correlation between planarity and irradiance applied to the sample surface. A too low irradiance causes low material ablation rates and insufficient generation of ions. Additionally, element fractionation can be observed since elements with an higher ionization potential are not ionized efficiently due to the lower plasma plume temperatures [20]–[22]. This leads to low signal-to-noise ratios (SNR) and incomplete chemical

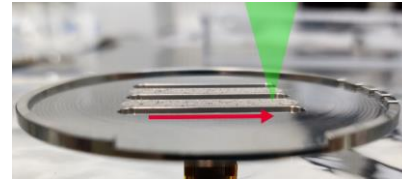


**Figure 6: The stainless steel sample holder filled with LHS-1 lunar analogue material to test the sample-handling concept on the laboratory LIMS prototype instrument. The laser beam is schematically depicted as green cone and the sample movement direction during measurement is indicated by the red arrow.**

information of the lunar regolith. On the other hand, a too high irradiance generates a too dense plasma at the ablation site as well as within the mass analyzer, resulting in space charge effects within the plasma plume and in the ion packets inside the analyzer, and thus reducing the mass resolution of the obtained spectra. This would make accurate chemical composition determination of the sample difficult.

The Gaussian beam propagation theory predicts a continuously increasing irradiance for a focused beam until the focus point is reached, after which the irradiance decreases again. To stay within an acceptable irradiance range for chemical analysis of the sample, the surface planarity must be appropriately controlled. Measurements using the laboratory setup were performed to determine the LIMS instrument's sensitivity regarding changes in laser irradiance  $I$ . Mass spectra at different laser pulse energies  $E$  were recorded and since  $I \sim E$ , direct correlations between  $I$  and spectral quality were obtained.

Figure 7 shows recorded mass spectra of LHS-1 at optimized laser irradiance (spectrum 1) and at 1.14x increased laser irradiance (spectrum 2), normalized to maximum signal intensity. The measurements were conducted while the sample was continuously moving underneath the mass

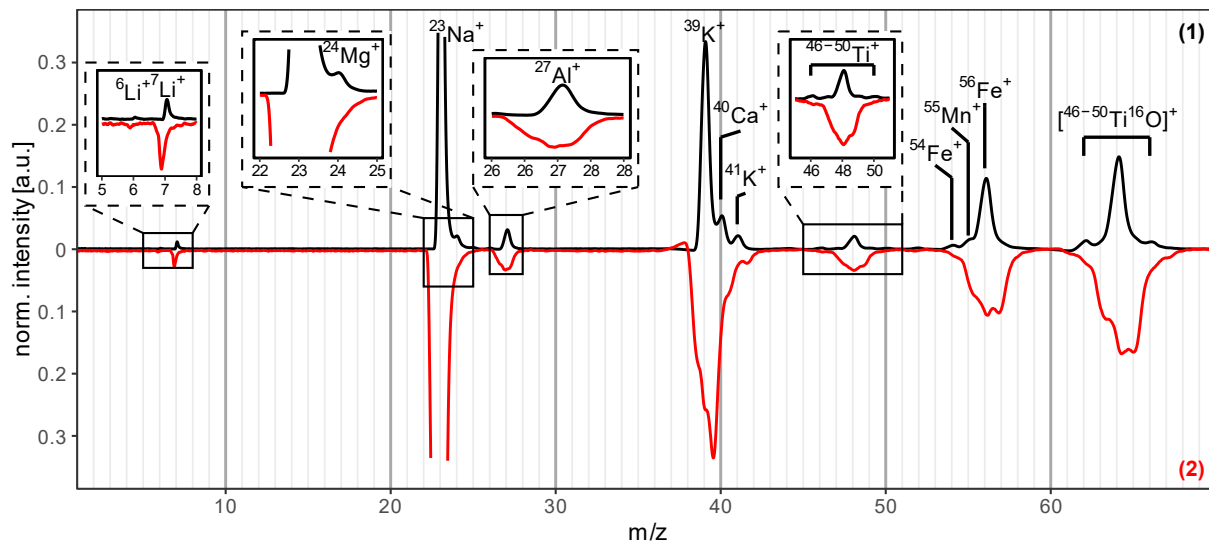


**Figure 7: Mass spectrum of LHS-1 lunar analogue material measured using the laboratory LIMS setup. The upper mass spectrum (1) has been recorded with an optimized laser pulse energy, whereas the lower (inverted) mass spectrum (2) was recorded with 1.14 times higher laser pulse energy. Degradation of the spectrum quality by peak broadening is visible.**

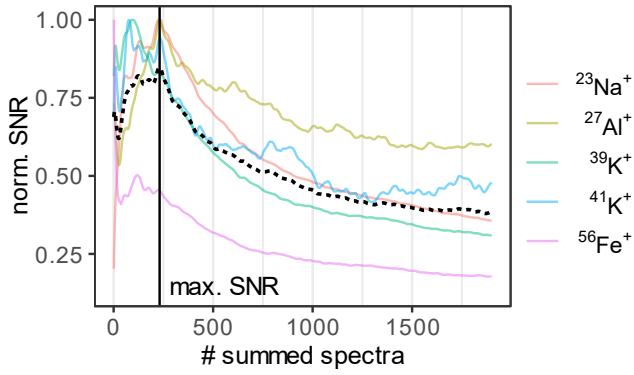


**Figure 8: Normalized SNR of selected species with increased number of laser shots fired. The spectra were recorded on a single position, without moving the sample. The dotted line depicts the equally weighted mean. The maximal SNR was reached after 231 shots as indicated by the vertical line.**

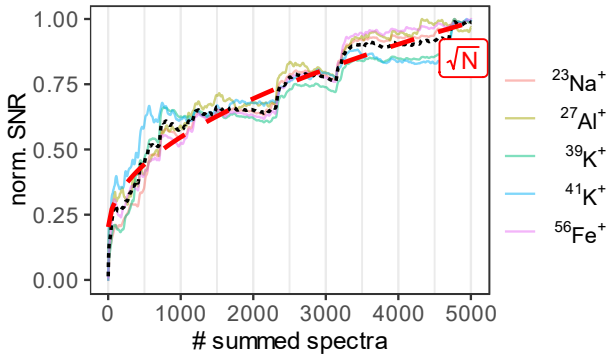


**Figure 9: Normalized SNR of different species for increasing number of laser shots while the sample is continuously moving. The dotted line depicts the mean SNR. The dashed line the shows theoretical increase of SNR with the square root of summed mass spectra ( $\sqrt{N}$ ).**

analyzer with a speed of  $\sim 0.8$  mm/s. The recorded single laser shot spectra were filtered to only include spectra with a  $^{23}\text{Na}^+$  signal having an SNR  $> 2$ . The filtered mass spectra were subsequently summed to obtain the final mass spectrum. For each energy level, about 5000 single shot spectra were recorded of which roughly 50 % matched the signal intensity criterion.

From the optimized spectrum (Figure 7, spectrum 1), all major elements present in LHS-1, except for Si and O, were detected. Additionally, peaks for some minor species, like  $^6\text{Li}^+$  and  $^7\text{Li}^+$  with the approximately correct isotope ratio of 1:10 are observed. These are not specified as compositing elements of LHS-1, since quantification by XRF, as used for the specification of LHS-1, is not able to detect Li. Mass spectrum (2), recorded with higher than optimal laser intensity, shows evident peak broadening. This masks the  $^{24}\text{Mg}^+$ ,  $^{41}\text{K}^+$ ,  $^{54}\text{Fe}^+$  and  $^{55}\text{Mn}^+$  peaks. Also, the isotopic structure of Ti is not discernible anymore.

From the known difference in laser irradiance between spectrum (1) and (2) and simulations of the laser beam propagation it can be derived that the sample planarity must

not change by more than  $\pm 0.3$  mm to ensure acceptable quality of the mass spectra. To allow for some safety margin, the sample planarity requirement was set to be  $\pm 0.2$  mm.

#### Sample movement speed during analysis

LIMS measurements are destructive to the sample within the area of analysis. Consecutive laser shots applied at the same sample location will create an ablation crater and thus will lead to signal degradation eventually. To prevent this, new sample material must be continuously presented to the instrument. The signal degradation with respect to the amount of applied laser shots is highly material dependent. Crater formation is slower for a compact solid than for a loose grainy substance such as LHS-1 or lunar regolith [23].

The goal of the presented measurements was to determine the minimally needed rotation speed of the carousel to always have enough fresh sample material at the analysis location. Therefore, the SNR of the mass spectrometric signal with respect to fired laser shots without moving the sample was investigated. Figure 8 shows such an SNR trace at optimized analysis conditions (i.e., optimized laser energy). The SNR has been normalized to correct for the different absolute signal intensities due to the species having different concentrations in the sample material. Thus, the dotted trace shows the equally weighted mean of the SNR. For the initial accumulation of 231 single-shot mass spectra, an increase in SNR was observed. After that, not enough sample material was present at the analysis location to generate high enough signal to further increase the SNR. Instead, more noise than signal was added to the summed spectra, leading to a decrease in SNR from that point on. This measurement was repeated 2 times, with the maximum normalized mean SNR being reached on average after 200 laser shots.

With the LIMS instrument's nominal laser frequency of 100 Hz, the sample must be advanced with an average speed of at least  $10 \mu\text{m/s}$  when a laser focus diameter of  $20 \mu\text{m}$  is assumed. A  $\sim 1$  Hz step frequency of the sample carousel's stepper motor is needed to reach this averages speed, as one step corresponds to  $14 \mu\text{m}$  of sample advancement with the chosen gearing (see Table 1).

Figure 9 shows the SNR trace of a control measurement conducted with the same laser parameters as before, but with the sample moving at a constant speed of  $\sim 0.8$  mm/s. With a continuously moving sample a decline in signal intensity is not observed. Consequently, the SNR continuously increases as more sample material is measured, closely following the theoretical SNR of  $\sqrt{N}$ , where  $N$  is the number of summed spectra.

#### Influence of the sample material's electrostatic charge

Regolith on the lunar surface is nominally electrostatically charged due to its exposure to solar UV radiation on the dayside, as well as the continuous stream of charged plasma particles impinging on the lunar surface [5]. The electrostatic potential on the sunlit surface ranges from a few volts positive up to  $+20$  V [24].

To guarantee accurate operation of the mass analyzer's ion optical system, no potential difference between the system's reference ground and the sample material shall exist. This is to avoid unwanted disturbances in the electric fields used by the mass analyzer's ion optical system to extract ions from the plasma plume generated during measurements. Due to the potential electrostatic charging of the lunar surface, and thus the regolith sample material, preventive measures must be taken. To this end, the funnel structure, including the sieves are electrically conducting, and connected to instrument ground. This is also valid for the SHS carousel, as well as the sample shaping brushes. This ensures that the static electrical charge of the supplied lunar regolith can dissipate and the potential difference between instrument ground and sample material is minimized. Vibration of the sample material during sieving, and the sample shaping process leads to a large contact area of the sample material with grounded structures, thus achieving maximized potential equilibration.

Laboratory experiments were conducted to assess the sensitivity of the ion optical system to charged sample material through the application of a bias voltage to the sample material via the sample holder. A cavity of the prototype instrument's sample holder was filled with LHS-1 regolith simulant. Instead of connecting the sample holder to instrument ground, the holder was electrically isolated and connected to a bipolar power supply. Measurements were

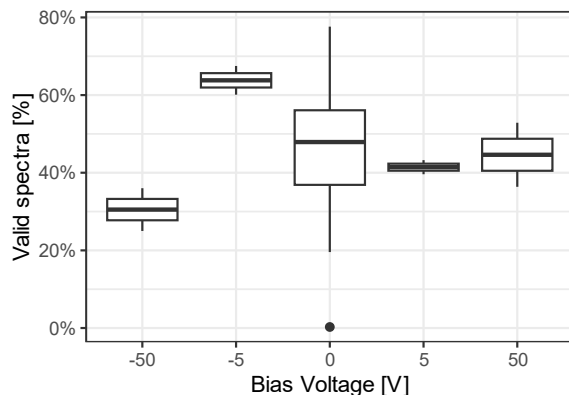


**Figure 10: Ratio of spectra with a  $^{23}\text{Na}^+$  signal of  $\text{SNR} > 2$  in dependence of applied bias voltage to simulate charged sample material.**

conducted while applying voltages of  $\pm 5$  V,  $\pm 10$  V and  $\pm 50$  V to the sample. Additionally, reference measurements were performed while the power supply output was set to 0 V. For analysis, the fraction of spectra having a mass peak of  $^{23}\text{Na}^+$  with an SNR of larger than 2 was calculated. The results are shown in Figure 10. All measurements with bias voltage applied are within the spread of the reference measurements conducted at 0 V.

Even at  $\pm 50$  V, which corresponds to more than twice the expected potential of the unequilibrated lunar regolith, no significant decrease in signal intensity was observed. The spectral quality did however decrease, but we are expecting to be able to compensate for this by re-tuning the ion optical system.

## 4. SUMMARY

We described a sample handling concept for the analysis of lunar regolith using laser ablation ionization mass spectrometry (LIMS). The current design for integrating this concept into our CLPS-LIMS instrument is shown. Laboratory LIMS measurements on regolith analogue material were conducted to evaluate the sample handling concept and guide the implementation thereof. Resiliency of the system to electrostatic charging of the lunar regolith has been demonstrated. A complete breadboard of the SHS is currently being built, for the final version to be a part of the LIMS instrument which is scheduled to fly to the lunar south pole region within the CLPS program.

## ACKNOWLEDGEMENTS

The financial support by the Swiss National Science Foundation and the Swiss Space Office is gratefully acknowledged.

## REFERENCES

- [1] P. Wurz, M. Tulej, A. Riedo, V. Grimaudo, R. Lukmanov, and N. Thomas, "Investigation of the Surface Composition by Laser Ablation/Ionization Mass Spectrometry," in *2021 IEEE Aerospace Conference (50100)*, Big Sky, MT, USA: IEEE, Mar. 2021, pp. 1–15. doi: 10.1109/AERO50100.2021.9438486.
- [2] Y. Langevin and J. R. Arnold, "The Evolution of the Lunar Regolith," *Annu. Rev. Earth Planet. Sci.*, vol. 5, no. 1, pp. 449–489, May 1977, doi: 10.1146/annurev.ea.05.050177.002313.
- [3] Y. Shkuratov, "Regolith Layer Thickness Mapping of the Moon by Radar and Optical Data," *Icarus*, vol. 149, no. 2, pp. 329–338, Feb. 2001, doi: 10.1006/icar.2000.6545.
- [4] G. H. Heiken, D. S. McKay, and R. W. Brown, "Lunar deposits of possible pyroclastic origin," *Geochim. Cosmochim. Acta*, vol. 38, no. 11, pp. 1703–1718, Nov. 1974, doi: 10.1016/0016-7037(74)90187-2.
- [5] T. J. Stubbs *et al.*, "Dependence of lunar surface charging on solar wind plasma conditions and solar irradiation," *Planet. Space Sci.*, vol. 90, pp. 10–27, Jan. 2014, doi: 10.1016/j.pss.2013.07.008.
- [6] N. Afshar-Mohajer, C.-Y. Wu, J. S. Curtis, and J. R. Gaier, "Review of dust transport and mitigation technologies in lunar and Martian atmospheres," *Adv. Space Res.*, vol. 56, no. 6, pp. 1222–1241, Sep. 2015, doi: 10.1016/j.asr.2015.06.007.
- [7] M. Tulej *et al.*, "CAMAM: A Miniature Laser Ablation Ionisation Mass Spectrometer and Microscope-Camera System for *In Situ* Investigation of the Composition and Morphology of Extraterrestrial Materials," *Geostand. Geoanalytical Res.*, vol. 38, no. 4, pp. 441–466, Dec. 2014, doi: 10.1111/j.1751-908X.2014.00302.x.
- [8] A. E. Chumikov, V. S. Cheptsov, P. Wurz, D. Lasi, J. Jost, and N. G. Managadze, "Design, characteristics and scientific tasks of the LASMA-LR laser ionization mass spectrometer onboard Luna-25 and Luna-27 space missions," *Int. J. Mass Spectrom.*, vol. 469, p. 116676,



Nov. 2021, doi: 10.1016/j.ijms.2021.116676.

- [9] U. Rohner, J. A. Whitby, and P. Wurz, "A miniature laser ablation time-of-flight mass spectrometer for *in situ* planetary exploration," *Meas. Sci. Technol.*, vol. 14, no. 12, pp. 2159–2164, Dec. 2003, doi: 10.1088/0957-0233/14/12/017.
- [10] U. Rohner, J. A. Whitby, P. Wurz, and S. Barabash, "Highly miniaturized laser ablation time-of-flight mass spectrometer for a planetary rover," *Rev. Sci. Instrum.*, vol. 75, no. 5, pp. 1314–1322, May 2004, doi: 10.1063/1.1711152.
- [11] A. Riedo, A. Bieler, M. Neuland, M. Tulej, and P. Wurz, "Performance evaluation of a miniature laser ablation time-of-flight mass spectrometer designed for *in situ* investigations in planetary space research: Miniaturised laser ablation tof mass spectrometer," *J. Mass Spectrom.*, vol. 48, no. 1, pp. 1–15, Jan. 2013, doi: 10.1002/jms.3104.
- [12] P. Wurz *et al.*, "In Situ Lunar Regolith Analysis by Laser-Based Mass Spectrometry," in *2023 IEEE Aerospace Conference*, Big Sky, MT, USA: IEEE, Mar. 2023, pp. 1–10. doi: 10.1109/AERO55745.2023.10115714.
- [13] V. Grimaudo *et al.*, "High-Resolution Chemical Depth Profiling of Solid Material Using a Miniature Laser Ablation/Ionization Mass Spectrometer," *Anal. Chem.*, vol. 87, no. 4, pp. 2037–2041, Feb. 2015, doi: 10.1021/ac504403j.
- [14] M. B. Neuland, S. Meyer, K. Mezger, A. Riedo, M. Tulej, and P. Wurz, "Probing the Allende meteorite with a miniature laser-ablation mass analyser for space application," *Planet. Space Sci.*, vol. 101, pp. 196–209, Oct. 2014, doi: 10.1016/j.pss.2014.03.009.
- [15] Exolith Lab, "LHS-1 Lunar Highlands Simulant Fact Sheet Dec. 2022." Dec. 2022. Accessed: Oct. 01, 2023. [Online]. Available: <https://cdn.shopify.com/s/files/1/0398/9268/0862/files/lhs-1-spec-sheet-Dec2022.pptx.pdf>
- [16] P. D. Spudis, B. Bussey, J. Plescia, J.-L. Josset, and S. Beauvivre, "Geology of Shackleton Crater and the south pole of the Moon," *Geophys. Res. Lett.*, vol. 35, no. 14, p. L14201, Jul. 2008, doi: 10.1029/2008GL034468.
- [17] J. K. Mitchell, W. N. Houston, R. F. Scott, N. C. Costes, W. D. Carrier III, and L. G. Bromwell, "Mechanical properties of lunar soil: Density, porosity, cohesion and angle of internal friction," *Lunar Planet. Sci. Conf. Proc.*, vol. 3, p. 3235, Jan. 1972.
- [18] Z. Khademian, E. Kim, and M. Nakagawa, "Simulation of Lunar Soil With Irregularly Shaped, Crushable Grains: Effects of Grain Shapes on the Mechanical Behaviors," *J. Geophys. Res. Planets*, vol. 124, no. 5, pp. 1157–1176, May 2019, doi: 10.1029/2018JE005889.
- [19] N. F. W. Ligterink *et al.*, "ORIGIN: a novel and compact Laser Desorption – Mass Spectrometry system for sensitive *in situ* detection of amino acids on extraterrestrial surfaces," *Sci. Rep.*, vol. 10, no. 1, p. 9641, Jun. 2020, doi: 10.1038/s41598-020-66240-1.
- [20] K. H. Lepore, M. D. Dyar, and C. R. Ytsma, "Effect of Plasma Temperature on Major Element Prediction Accuracy From Laser-Induced Breakdown Spectroscopy," *Geophys. Res. Lett.*, vol. 50, no. 8, p. e2023GL102919, Apr. 2023, doi: 10.1029/2023GL102919.
- [21] L. Torrisi, "Fractional ionization in plasmas produced by pulsed laser ablation," *Radiat. Eff. Defects Solids*, vol. 157, no. 3, pp. 347–356, Jan. 2002, doi: 10.1080/10420150212994.
- [22] R. Huang *et al.*, "High irradiance laser ionization orthogonal time-of-flight mass spectrometry: A versatile tool for solid analysis," *Mass Spectrom. Rev.*, vol. 30, no. 6, pp. 1256–1268, Nov. 2011, doi: 10.1002/mas.20331.
- [23] S. Wu, V. Karius, B. C. Schmidt, K. Simon, and G. Wörner, "Comparison of Ultrafine Powder Pellet and Flux-free Fusion Glass for Bulk Analysis of Granitoids by Laser Ablation-Inductively Coupled Plasma-Mass Spectrometry," *Geostand. Geoanalytical Res.*, vol. 42, no. 4, pp. 575–591, Dec. 2018, doi: 10.1111/ggr.12230.
- [24] M. A. Fenner, J. W. Freeman Jr., and H. K. Hills, "The electric potential of the lunar surface," *Lunar Planet. Sci. Conf. Proc.*, vol. 4, p. 2877, Jan. 1973.

## BIOGRAPHY



**Peter Keresztes Schmidt** received his B.Sc. and M.Sc. in Chemistry at the ETH Zürich, Switzerland. He is currently working as a PhD student in Bern, Switzerland, where he is developing a new the LIMS instrument for *in situ* studies on the lunar surface.



**Sébastien Hayoz** gained experience in different fields like electronics' development for Automotive, electronics' systems for Train Control Monitoring System (TCMS). Since February 2021, he is leading the electronics engineering team at the Space Research and Planetary Division and is involved for several instruments realized by the University of Bern.



**Daniele Piazza** has more than 20 years of experience in the design and development of space instruments. He has a Ph.D. in mechanical engineering from ETH Zurich and started his career in Formula 1. Since 2005 he leads the mechanical engineering group working on space instruments at the University of Bern.



**Timothy Bandy** has B.Sc. degree in mechanical engineering. He has mainly worked in the defense, pharmaceutical fields before joining UBE. Since then, he supported the development and AIV of BELA (BepiColombo), CHEOPS and CometInterceptor. He is now Systems Engineer for CLPS-LIMS.



**Patrik Mündli** received a M.Sc. in electrical engineering and information technology, ETH Zurich, Switzerland. For 7 years he worked in control, network and communications technology for all types of rail vehicles. Since March 2022, he is system engineer electronics for CLPS-LIMS.



**Matthias Blaukovitsch** has a M.Sc. in Physics from the Technical University of Vienna, Austria (2016). He has been working on time-of-flight sensors specializing on diode lasers and is now appointed as an optical engineer at the University of Bern.



**Michael Althaus** received a HTL & B.Sc. in Electrical Engineering from Lucerne University of Applied Sciences and Arts with specialization in Information Technology in 1999. He worked as a research engineer at ESEC SA in Switzerland and at the Centre for Advanced Materials Joining, University of Waterloo, Canada. Before joining the

University of Bern in 2018 for the NIM (JUICE), the NGMS (Luna 27) and – lately – the CLPS-LIMS instruments, he worked as an R&D Senior SW/HW engineer in the industry.



**Benoît Plet** received his Ph.D. in Physical Chemistry from the University of Bordeaux, France, in 2007. After 15 years developing scientific instrumentation in industry, he has joined University of Bern, Switzerland, as project manager.



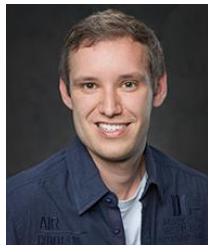
**Sven Riedo** received a B.Sc. in Electrical Engineering in 2022 from the University of Applied Sciences and Arts Western Switzerland. He is currently working as an electronic engineer at the University of Bern.



**Simon Studer** received his B.Sc. in Automotive Engineering in 2013 from the University of Applied Sciences Bern, Switzerland. He spent most of his time in Formula 1 before he joined as Mechanical Engineer to the Space Research and Planetary Sciences group of the University Bern.



**Olivier Studer** received his M.Sc. in Mechanical Engineering in 2023 from the University of Applied Sciences and Arts Northwestern Switzerland. Since September 2023 he is working as a mechanical design engineer on the sample handling system of CLPS-LIMS.



**Michael Bieri** received a B.Sc. in Electrical Engineering and Information Technology from the University of Applied Sciences Bern, Switzerland in 2022. Since Oct. 2022 is working at the University of Bern as software and electronics engineer on CLPS-LIMS and NGMS / Luna 27.



**Marek Tulej** received a Ph.D. in Physical Chemistry from the University of Basel, Switzerland in 1999. After his post-doctoral period at Paul Scherrer Institute (PSI), Switzerland, he joined in 2008 the University of Bern as an instrument scientist for space missions, including Phobos-Grunt, Marco Polo-R, Luna-Resurs, and JUICE.



**Andreas Riedo** received his Ph.D. in Physics in 2014 from the University of Bern, Switzerland. In 2016 he received a SNSF fellowship that allowed him to continue his research in Astrobiology at the Leiden University, The Netherlands. He extended his stay at the Leiden University with a MCSA fellowship for another two years before he moved in

2019 to the Free University Berlin after receiving the Einstein fellowship. In 2020 he moved to University of Bern and is currently appointed as researcher and project leader for CLPS-LIMS.



**Peter Wurz** has a degree in electronic engineering (1985), an M.Sc. and a Ph.D. in Physics from Technical University of Vienna, Austria (1990). He has been a post-doctoral researcher at Argonne National Laboratory, USA. Since 1992 at the University of Bern. He is Professor of physics, 2015–2022 head of the Space Science and Planetology division, and since 2022 director of the physics institute. He has been Co-I and PI for many science instruments for space missions of ESA, NASA, ISRO, CNSA, Roscosmos, and JAXA.